Sensors and Actuators A 189 (2013) 335–338

Contents lists available at SciVerse ScienceDirect

Sensors and Actuators A: Physical

journal homepage: www.elsevier.com/locate/sna

Acoustic whispering gallery mode coupling with Lamb waves in liquid

Feng Li[a], Ming Xuan[a], Yihui Wu[a,*], François Bastien[b]

[a] State Key Laboratory of Applied Optics, Changchun Institute of Optics, Fine Mechanics and Physics, Chinese Academy of Sciences, Changchun 130033, China
[b] FEMTO-ST Institute, MN2S Department, CNRS-UMR 6174, Besançon, France

ARTICLE INFO

Article history:
Received 31 October 2011
Received in revised form 3 September 2012
Accepted 21 October 2012
Available online 30 October 2012

Keywords:
Whispering gallery mode
Lamb wave

ABSTRACT

Acoustic whispering gallery modes (WGMs) in a micro-quartz tube immersed in liquid medium, excited by the evanescent wave of a Lamb wave device, are demonstrated. These excited WGMs exhibit characteristics similar to those of optical WGMs, such as narrow periodic transmission dips and a high quality factor. These results show the possibility to build acoustic sensors, filter and acoustic resonators working in liquid with improved performance.

1. Introduction

Lord Rayleigh discussed the whispering galleries in buildings about 100 years ago. In recent years, the notion of the whispering gallery mode (WGM) extended from acoustics to optics. The WGMs of micro-spheres or micro-disks confine the light in a narrow ring along the equator of the structure by total internal reflection at the resonator surface. The WGMs show extremely high quality factors ($Q > 10^8$) and a small mode volume [1–4]. It finds lot of applications, including laser [5], optical filter [6], biosensor [7], etc. Recently the interaction between optics WGMs and acoustics/mechanics was investigated [8–12]. It is interesting to show that the optics WGMs can either excite or extinct the mechanical vibration of small resonators.

The pure mechanical wave on circular structure can have high Q factors due to their closed structures. For example, the wineglass mode resonators exhibit extremely high Q factor and have many applications [13]. Hopefully, acoustic WGMs on circular structures can also exhibit a high Q factor and other characters as the optical device. The circumferential waves in the tube have been investigated by exciting and measuring the tube with PZT directly [14]. It shows the sensitivity to the liquid filled in the tube. However, the original acoustic WGMs were relatively rarely investigated, especially in micro-ring resonators or coupled with evanescent waves. Contrary to high Q resonator with Rayleigh wave in air or vacuum, Rayleigh wave on the resonator loaded with liquid will attenuate a lot due to wave leakage into the liquid. As for the Lamb wave in membrane loaded with liquid, there is no leaky wave if their phase velocity is lower than the sound velocity of the loading liquid [15]. Thus high Q factor acoustic WGMs in liquid can be obtained based on Lamb wave resonator.

In the current study, we investigated a micro-acoustic WGM, which were excited and measured by evanescent wave from Lamb wave device. The characteristics of acoustic WGMs were studied both theoretically and experimentally. It is shown that acoustic WGMs can also have narrow periodic dips such as optical WGMs due to the closed circular structure of the tube. Thus the high Q factor of acoustic WGMs was obtained. Furthermore, the resonance frequency shifts due to the mass changing on the tube surface was measured. These results can be used in designing acoustic resonator, filter and sensors.

In the case of optical WGMs, the evanescent wave extends out from the taper optical fiber and couples with micro-optical cavities [4]. Evanescent wave of Lamb wave device loaded with liquid will penetrate into liquid if the phase velocity of Lamb wave is less than sound velocity of the liquid. Instead of using micro-spheres or micro-disks as optical WGMs, a thin wall tube was adopted because it will not leak acoustic energy significantly into liquid when the phase velocity of the tube is less than sound velocity of the liquid. If the tube enters the evanescent region and the working frequency of the Lamb wave device overlaps with the resonant frequency of the tube, the Lamb wave device will couple with the tube via the evanescent wave.

2. Setup of experiments

The experimental scheme for the acoustic WGMs is shown in Fig. 1. The Lamb wave device is loaded with water at the upper

* Corresponding author. Tel.: +86 43186176915.
E-mail address: ciomp_yihuiwu@hotmail.com (Y. Wu).

0924-4247/$ – see front matter © 2012 Elsevier B.V. All rights reserved.
http://dx.doi.org/10.1016/j.sna.2012.10.028

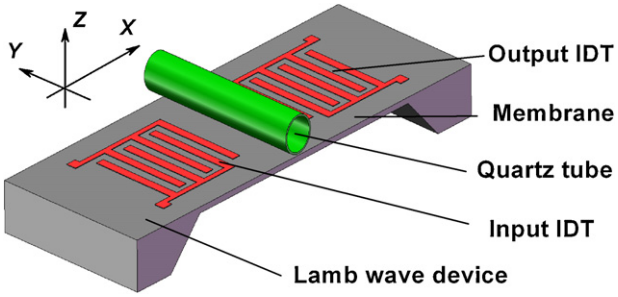

Fig. 1. Principle of the acoustic WGMs system.

side and the water depth is much larger than the Lamb wave wavelength. An empty fused quartz tube is located above the Lamb wave device, with a distance close to the evanescent wave penetration depth. One pair of interdigital transducer (IDT) is connected to the output of a gain-phase analyzer (Agilent 4395A) and excites the Lamb wave on the membrane. The Lamb wave propagates on the membrane and transforms into an electrical signal into another IDT. The Lamb wave propagates in the X direction and couples with the tube, which resonates in the circumferential direction. The electrical signal is then measured by the gain-phase analyzer. Hopefully, the acoustic WGMs can be measured from the output IDT.

Acoustic WGMs in a fused quartz tube were excited and measured using a Lamb wave device, which was fabricated under clean room conditions. The thickness of the silicon membrane is 18 μm and its dimension is 8 mm × 8 mm; two pairs of IDT were built on a 2 μm piezoelectric aluminum nitride (AlN) layer, with a spatial period of 400 μm. The process steps used to fabricate the Lamb wave device are listed as follows (shown in Fig. 2): (a) lithography on silicon dioxide wafer and defining etching area for membrane; (b) aligning mark etching and etching the membrane until 18 μm; (c) removing the silicon dioxide; (d) sputtering aluminum for electric ground layer; (e) sputtering piezoelectric AlN; (f) fabricating IDT by lift-off process. The quartz tube was purchased from Charles Super Company. The diameter of the tube is 1.0 mm, the length is 50 mm, and the thickness of the wall is 20 μm.

The picture of the acoustic WGMs device is shown in Fig. 3. During the measurement, the Lamb wave device is loaded with water and covered by a glass above. The distance between the tube and the Lamb wave device can be adjusted precisely by the stage.

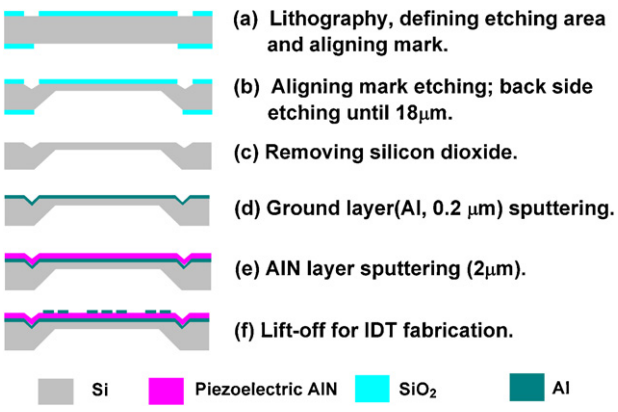

Fig. 2. The fabrication processes of the Lamb wave devices.

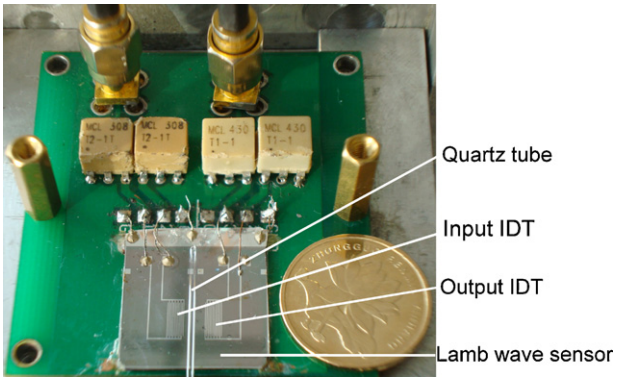

Fig. 3. The picture of acoustic WGMs system.

3. Calculations and experimental results

3.1. The frequencies of acoustic WGMs

When the tube resonates in circumferential direction, the wavelength takes discrete values:

$$L = m \cdot \lambda \quad (1)$$

where m is an integer and L is the circumference of the tube. The waves in the tube and water can be analyzed with polar coordinates [16]. The waves in the tube and in the liquid can be expressed using Bessel functions. Three boundary conditions exist at the external liquid tube interface, namely continuity of the normal stress, the normal displacement, and zero shear stresses. Two boundary conditions exist at the internal solid–air interface, namely the zero tangential and normal stresses. The eigen frequencies of the WGMs are obtained by solving the eigenfunction using these boundary conditions. The resonant frequencies of acoustic WGMs corresponding to m number are plotted in the panel of Fig. 4.

With network analyzer, a wide transmission peak of the Lamb wave is observed from 0.5 to 1.7 MHz (Fig. 4). The evanescent wave excited by the Lamb wave device penetrates into the liquid. When the tube is moved into the evanescent field region, the Lamb wave traveling through the Lamb wave device is coupled with the WGMs. The Lamb wave transmissions with two different distances between the device and the tube (120 μm and 200 μm) are plotted in Fig. 4, respectively. Several narrow dips are observed when the distance is 120 μm. The resonances of the tube were identified from the frequencies of these periodic dips. The experimental frequencies of acoustic WGMs corresponding to each m are also plotted in

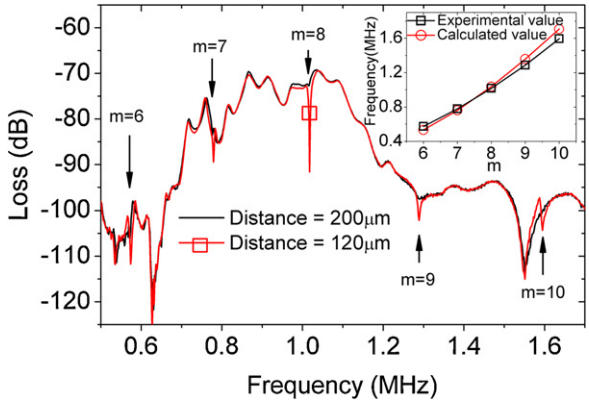

Fig. 4. Responses of the acoustic WGMs with different distances between the Lamb wave device and the tube.

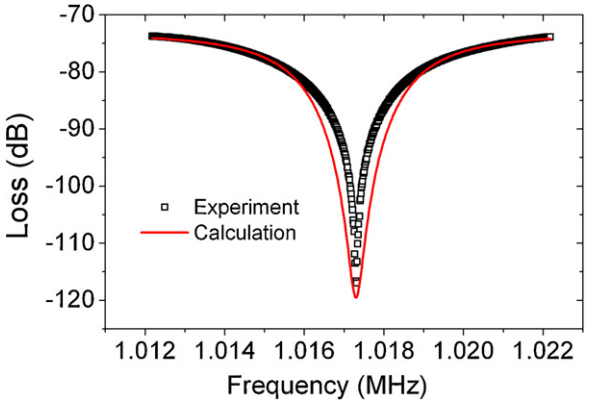

Fig. 5. Experimental and calculated transmission losses of the acoustic WGMs near the critical coupling condition.

the same panel of Fig. 4 and agree with the experimental values well.

3.2. The response of acoustic WGMs

To determine the transmission of the acoustic wave, the WGMs were analyzed using the circulated and ballistic Lamb waves similar to optical WGM analysis [17]. A part of the incident Lamb wave does not couple with the tube but directly propagates to the output IDT and is referred to as ballistic wave. The Lamb wave circulating though the tube also emerges as an evanescent wave and again couples with the Lamb wave device. The output is the interferences between the circulated and the ballistic waves. Using the formula for optical WGMs, the transmission coefficient can be expressed as follows [17]:

$$C = \left| \frac{\tau - \exp(-i\theta)}{1 - \tau \cdot \exp(-i\theta)} \right| \tag{2}$$

with

$$\theta = \left(\frac{2\pi}{\lambda} - i\alpha \right) 2\pi \cdot r \tag{3}$$

where α is the attenuation factor due to intrinsic losses in the tube, τ is the through amplitude coupling constant of the coupler, λ is the wavelength in the tube, and r is the radius of the tube.

For $m = 8$, $C(\tau, \alpha)$ in Eq. (2) gives low values along the $\alpha = 342(1 - \tau)$ line. If a base line of −73 dB and $\tau = 0.962$ are used, the transmission from Eq. (2) is obtained. The calculated transmissions are plotted in Fig. 5 and agree with the experimental results.

The transmissions corresponding to the different distances between the tube and the Lamb wave device were measured (Fig. 6). The curve shows the redistribution of the input power when the distance is adjusted. When the distance is 85 μm, the WGMs are over-coupled. When the distance is 125 μm, the transmission is near zero. When the distance is further increased, the WGMs become under-coupled.

The Q factors of the WGMs were obtained from the bandwidth of the dip and plotted in Fig. 6. As the coupling distance is increased, the Q factor increases because of the lower coupling loss. When the distance is 200 μm, the Q factor of the WGMs reaches 380, which is one order higher than that of the Lamb wave device working in liquid.

3.3. The sensitivity of acoustic WGMs to mass changing

Optical WGMs have been proved to be extremely sensitive to the optical refractive index changes on the surface of optical micro-cavity and this new sensor can even detect single molecule

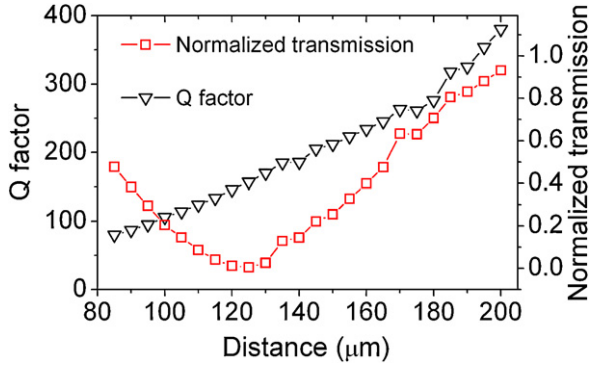

Fig. 6. Normalized transmission and Q factors with different coupling distances.

[8]. Acoustic sensor, such as Lamb wave sensor, quartz crystal microbalance (QCM), can detect the mass changes attached to the sensor's surface by reading the frequency shifts. As for acoustic WGMs, the frequency of the dip also shifts when the mass attaches to the tube's surface. The variations in the frequency shift Δf due to the mass change Δm can be expressed as follows [18]:

$$\frac{\Delta f}{f} = S \cdot \Delta m \tag{4}$$

The sensitivity of the WGMs is:

$$S = -\frac{1}{2} \frac{1}{\rho_t h + \rho_l \delta} \tag{5}$$

where ρ_t and ρ_l are the densities of the tube and the liquid, respectively, h is the thickness of the tube, and δ is the evanescent wave penetration depth. For a 20 μm thick tube with $m = 8$, the theoretical evanescent wave penetration depth is approximately 63 μm. Using Eq. (5), the theoretical mass sensitivity is 46.7 g^{-1} cm^2.

Mass changes accompanying electrochemical reactions can be accurately measured from the frequency shifts of the dips. The copper electroplating was used on the tube surface and the mass changing experiment conducted is similar to Ref. [18]. The copper electroplating principle is expressed by:

$$Cu^{2+} + 2e^- \rightarrow Cu \tag{6}$$

The mass changing of copper on the surface of the quartz tube was controlled by the electric current, which is the square wave at a period of 100 s (Fig. 7). When the current is about 3.68×10^{-4} A, copper begins to deposit on the surface of the tube; when the current is zero, copper deposition stops. From the deposition time and electric current, the total mass of copper on the tube is known.

The frequency shifts of the 8th WGM dips due to copper deposition with time are plotted in Fig. 7. The frequency decreased during copper deposition. The mass sensitivity of WGMs can be

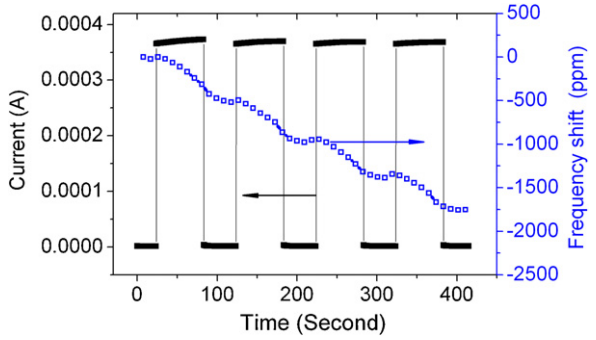

Fig. 7. The frequency of WGM of the tube decreases when the copper is deposited on the tube.

obtained from Eq. (3). The measured sensitivity of the 8th WGM is 32.4 g^{-1} cm^2, which agrees with the theoretical mass sensitivity.

The performance of a given noise acoustic sensor is mainly influenced by the sensitivity and the Q factor. The minimum mass resolution is given by the figure of merit (FOM) [19], which is expressed as

$$\mathrm{FOM} = \frac{1}{S \cdot Q} \tag{7}$$

A lower FOM value means a higher mass resolution. Considering that the Q factor of the WGM is one order higher than that of the Lamb wave sensor, the minimum detectable mass is decreased by one order compared with a Lamb wave sensor with the same thickness.

4. Conclusion

In conclusion, acoustic WGMs in a fused quartz tube immersed in water was excited and measured by putting the tube in the evanescent field region of a Lamb wave device. The acoustic WGMs in micro-resonators exhibit characteristics similar to those of optical WGMs. The acoustic WGMs exhibited sharp periodic dips due to the resonance of the circular structure of the tube. It was proved that the acoustic WGMs are sensitive to the mass changing on the resonator's surface. The Q factor of the acoustic WGMs reaches 380, which is one order higher than that of the Lamb wave device working in liquid. Therefore, the resolution of mass change was improved comparing with Lamb wave sensors.

Furthermore, for acoustic WGMs the resonator is isolated from the excitation region thanks to the evanescent wave coupling; a versatile acoustic WGMs array can be fabricated. These conclusions will help to design new acoustic resonators, sensors or filters.

Acknowledgements

This work is supported by a Natural Science Foundation of China (60871043, 60971025, and 11034007) and the Key Knowledge Innovation Project of the Chinese Academy of Sciences (KJCX2-YW-H18).

References

[1] M.L. Gorodetsky, A. Savchenkov, V.S. Ilchenko, Ultimate Q of optical microsphere resonators, Optics Letters 21 (1996) 453–455.
[2] I.S. Grudinin, V.S. Ilchenko, L. Maleki, Ultrahigh optical Q factors of crystalline resonators in the linear regime, Physical Review A 74 (2006) 063806.
[3] D.K. Armani, T.J. Kippenberg, S.M. Spillane, K.J. Vahala, Ultra-high-Q toroid microcavity on a chip, Nature 421 (2003) 925–928.
[4] M. Cai, O. Painter, K.J. Vahala, Observation of critical coupling in a fiber taper to a silica-microsphere whispering-gallery mode system, Physical Review Letters 85 (2000) 74–77.
[5] K. Kieu, M. Mansuripur, Fiber laser using a microsphere resonator as a feedback element, Optics Letters 32 (2007) 244–246.
[6] L. Maleki, A.B. Matsko, A.A. Savchenkov, V.S. Ilchenko, Tunable delay line with interacting whispering-gallery-mode resonators, Optics Letters 29 (2004) 626–628.
[7] A.M. Armani, R.P. Kulkarni, S.E. Fraser, R.C. Flagan, K.J. Vahala, Label-free, single-molecule detection with optical microcavities, Science 317 (2007) 783–787.
[8] A.B. Matsko, A.A. Savchenkov, V.S. Ilchenko, D. Seidel, L. Maleki, Optomechanics with surface-acoustic-wave whispering-gallery modes, Physical Review Letters 103 (2009) 257403.
[9] A.A. Savchenkov, A.B. Matsko, V.S. Ilchenko, Surface acoustic wave optomechanical oscillator and frequency comb generator, Optics Letters 36 (2011) 3338–3340.
[10] J. Zehnpfennig, G. Bahl, M. Tomes, T. Carmon, Surface optomechanics: calculating optically excited acoustical whispering gallery modes in microspheres, Optics Express 19 (2011) 14240–14248.
[11] G. Bahl, J. Zehnpfennig, M. Tomes, T. Carmon, Stimulated optomechanical excitation of surface acoustic waves in a microdevice, Nature Communications 2 (2011) 403.
[12] G. Bahl, M. Tomes, F. Marquardt, T. Carmon, Observation of spontaneous Brillouin cooling, Nature Physics 8 (2012) 203–207.
[13] J.E.-Y. Lee, A.A. Seshia, 5.4-MHz single-crystal silicon wine glass mode disk resonator with quality factor of 2 million, Sensors and Actuators A 156 (2009) 28–35.
[14] X. Li, J.D.N. Cheeke, Z. Wang, C.K. Jen, M. Viens, G. Yi, M. Sayer, Ultrasonic thin-walled tube wave devices for sensor applications, Applied Physics Letters 67 (1995) 37–39.
[15] F. Li, Y. Wu, J.-F. Manceau, F. Bastien, Measurements of evanescent wave in a sandwich Lamb wave sensor, Applied Physics Letters 92 (2008) 074101.
[16] J.L. Rose, Ultrasonic Waves in Solid Media, Cambridge University Press, 1999 (Chapter 12).
17 H.P. Uranus, H.J.W.M. Hoekstra, Modeling of loss-induced superluminal and negative group velocity in two-port ring-resonator circuits, Journal of Lightwave Technology 25 (2007) 2376–2384.
[18] H. Jia, R. Duhamel, J.-F. Manceau, M. de Labachelerie, F. Bastien, Improvement of Lamb waves sensors: temperature sensitivity compensation, Sensors and Actuators A 121 (2005) 321–326.
[19] J. Weber, W.M. Albers, J. Tuppurainen, M. Link, R. Gabl, W. Wersing, M. Schreiter, Shear mode FBARs as highly sensitive liquid biosensors, Sensors and Actuators A 128 (2006) 84–88.